BNL-79212-2007-JA

DETERMINATION OF CLOUD LIQUID WATER DISTRIBUTION USING 3D CLOUD TOMOGRAPHY

D. Huang[1]*, Y. Liu[1] , and W. Wiscombe[2]

July 2007

Submitted for publication in
Journal of Geophysical Research

Environmental Sciences Department/Atmospheric Sciences Division

Brookhaven National Laboratory
P.O. Box 5000
Upton, NY 11973-5000
www.bnl.gov

[1] Brookhaven National Laboratory, Atmospheric Sciences Division, Upton, NY 11973-5000
[2] NASA Goddard Space Flight Center (code 913), Greenbelt, MD 20771

*Author for correspondence: Dong Huang, Atmospheric Sciences Division, Environmental Sciences Department, Brookhaven National Laboratory, Building 815E, 75 Rutherford Dr., Upton, NY 11973; Tel: (631) 344-5818; email: dhuang@bnl.gov.

Abstract

The 3D distribution of cloud liquid water content is needed in many areas. The cloud microwave tomography method for remotely retrieving 3D distributions of cloud Liquid Water Content (LWC) was originally proposed by Warner et al. in the 1980s but has lain dormant since then. This paper revisits and extends the cloud tomography method by rigorously examining the nature of the resultant mathematical problem and its close relationship to the physical configuration of microwave radiometers. The mathematical analysis reveals that the retrieval of cloud LWC fields from microwave emission is highly ill-posed, and requires special methods to solve it. The ill-posed nature of the problem is examined by means of singular value decomposition (SVD), and the truncated SVD along with the L-curve method is used to obtain the optimal retrieval of cloud LWC. Sensitivity studies show that the retrieval accuracy is determined by several factors, including the number of radiometers, the number of scanning angles, the noise level of the radiometers, and the spatial resolution of the output. When more radiometers and/or more scanning angles are used, and/or when a coarser output resolution is acceptable, the retrieval problem becomes less ill-posed, and a better retrieval can be obtained. Furthermore, the Observation System Simulations demonstrate that the cloud tomography method is able to retrieve the cloud structures generated by cloud resolving models with a good accuracy. For a setup consisting of 4 microwave radiometers of typical noise level 0.3 K, the tomography method is capable of retrieving the LWC to within 5% of the maximum LWC in the simulated stratocumulus and broken cumulus cases, with a spatial resolution of a few hundred meters.

1. Introduction

Clouds in the lower troposphere are an important component of the hydrologic cycle, and also exert an enormous influence on the Earth's radiation budget. Consistent observations of clouds are needed in many relevant areas such as weather forecasting and climate modeling, and have received a lot of attention in the past several decades. For example, the overarching goal of the Atmospheric Radiation Measurement (ARM) program is to improve this representation of cloud and radiation in climate models, partly by providing long-term consistent data products (Ackerman and Stokes, 2003). For more than 10 years, ARM has been collecting data related to radiation and clouds at three primary sites representing a wide range of climatic conditions. Despite the great efforts, spatial distribution of cloud water, a key aspect of clouds, is still one of the largest uncertainties in global climate models (Stephens, 2005). Part of the reason is that existing techniques are difficult to provide a full view of clouds: they either sample a small volume of a cloud or measure only the vertical integral of the Liquid Water Content (LWC). For example, in situ measurements employ hot wires or optical probes on an aircraft to determine LWC. The sample volume of such techniques is so small that it would take thousands of years to measure an entire cloud (Wiscombe, 2005). On the other hand, remote sensing techniques like dual-frequency cloud radar (Hogan et al., 2005) with rapid scanning capability seems promising, but they are too costly for the community.

Single microwave radiometers have been widely used in passive remote sensing to measure cloud liquid water and water vapor (Westwater et al., 2004). They mainly provide path-integrated amounts since they have poor resolution along the measurement

path. To improve on their spatial resolution, microwave tomography methods were proposed by Warner et al. (1985, 1986, 1988), Twomey (1987), and Drake and Warner (1988). Tomography has been widely used in different disciplines such as medical imaging, archaeology, biology, geology, astronomy, and oceanography. Perhaps one of the most famous applications is the X-ray transmission computed tomography used for imaging the internals of a human body. Tomography is also found useful in imaging the Earth's atmosphere: Fleming (1982) and Hoffman et al. (1989) simulated retrieving cross sections of the vertical atmospheric temperature structure from satellite radiance measurements taken at various angles and frequencies; Flores et al. (2000) retrieved the tropospheric water vapor distribution using the wet delay data derived from a locally dense network of GPS receivers.

Warner et al. (1985, 1986) pioneered cloud tomography using two microwave radiometers to determine the spatial distribution of cloud LWC. Their setup involved planar-scanning a cloud with two ground-based 31-GHz radiometers, although, in six weeks of scanning, only one cloud passed between the two radiometers that could yield a credible tomographic retrieval. Their retrieval algorithm, non-negative least squares, was that of Lawson and Hanson (1974). The simulation studies demonstrated that cloud tomography was capable of estimating LWC to within 10% of the maximum LWC with a spatial resolution of a few hundred meters. Twomey (1987) developed an iterative non-linear inversion algorithm for tomographic problems to reduce the computation cost, which was a major limit at that time. Drake and Warner (1988) performed computer simulations of tomographic retrieval of cloud LWC with an airborne radiometer, and their retrieval algorithm was similar to that of Warner et al. (1985). A field test of this

setup was carried out in Louisiana and the LWC deduced from the radiometric measurements showed statistically good agreement with that measured directly by an airborne Particle Measurement System (Warner and Drake, 1988).

Unfortunately, the cloud tomography subject has lain dormant since the pioneering works, leaving some important questions unanswered. For example, the mathematical nature of the cloud tomography retrieval problem and its relationship to the physical configuration has not been rigorously examined, although they are essential for optimizing the retrieval algorithm and for determining the best physical arrangement and scanning strategy. In the intervening 20 years, many advances have been made in the relevant areas (e.g., smaller, cheaper and more efficient microwave radiometer technology; more realistic 3D cloud-resolving models; better mathematical methods for ill-posed problems; and faster computer speed), permitting a better investigation of the cloud tomography technique. For example, Figure 1 shows the evolution of the old-days dual-frequency radiometers used in Warner et al. (1986) to the nowadays multi-frequency Ground-based Scanning Radiometer. Not only have the radiometers become much more mobile, but also the calibration technique has been advanced from the tipping curve calibration using one blackbody reference (Hogg et al., 1983) to the more accurate calibration method using two external blackbody references (Westwater et al., 2004). Over the same period, more realistic 3D cloud-resolving models have emerged, better mathematical tools for ill-posed problem have been developed, and much faster and cheaper computers have been made available. Together with the need for measuring 3D distribution of cloud water content, a renaissance of the cloud tomography is now timely.

This paper revisits the cloud tomography technique, and discusses several improvements on the tomography setup of Warner et al. (1985). The paper also rigorously examines the mathematical nature of the retrieval problem, specifically its ill-posedness, and demonstrates the combination of the truncated singular value decomposition (SVD) method and the L-curve method to obtain optimal retrievals. The paper is organized as follows. Section 2 provides a description of the theoretical formulation of the cloud tomography method. Section 3 elaborates the mathematical nature of the tomographic retrieval problem. Section 4 shows some Observing System Simulations of cloud tomography including sensitivity studies. A summary of the findings in this study and discussions on improving and extending cloud tomography are given in Section 5.

2. Observing System Simulation for Cloud Tomography

Observing System Simulation Experiment (OSSE) is a useful tool to study a forecast or retrieval system. The OSSE for cloud tomography mainly contains two components: a forward model to generate the atmosphere state and simulate the microwave measurements, and an inverse algorithm to retrieve the cloud water field from the simulated microwave data. Specifically, the forward model first generates the atmosphere state variables using a cloud resolving model (Section 4), then computes the microwave measurements using the radiative transfer equation.

The radiative transfer equation relating the microwave radiation intensity to the atmosphere state is:

$$I(\Omega_i) = I_\infty \tau(\Omega_i, 0, \infty) + \int_0^\infty B(T)\alpha(s, \Omega_i)\tau(\Omega_i, 0, s)ds\,, \qquad (1)$$

where $I(\Omega_i)$ is the intensity of radiation reaching a radiometer from direction Ω_i; I_∞ is the intensity of the cosmic background radiation; $B(T)$ is the Planck function at temperature T; α is the absorption coefficient determined by the atmosphere state; and $\tau(\Omega_i, s_1, s_2) = \exp[-\int_{s_1}^{s_2} \alpha(s, \Omega_i)ds]$ is the transmission between two points s_1 and s_2 along direction Ω_i. Since transmission decreases along photon path, emission signal from clouds far from the radiometer is likely to be severely attenuated by the atmosphere. Therefore, we restrict cloud tomography to map the cloud structure over a field of 5 km by 5 km. Furthermore, very large zenith angles (>85°) are excluded in our simulations to avoid very long photon path in the low troposphere.

For ice-free clouds (ice would add the complication of scattering), cloud tomography measures the line integrals of cloud emission along many directions. These integrals are related to the spatial distribution of cloud absorption coefficients by the microwave radiative transfer equation (Eq. (1)) and are measured by the microwave radiometers. A radiometer measurement $\bar{I}$ is the convolution of I with the antenna gain pattern G, which usually deceases exponentially with the square of angular departure from the center axis Ω_i (Drake and Warner, 1988),

$$\bar{I}(\Omega_i) = \int I(\Omega)G(\Omega - \Omega_i)d\Omega\,. \qquad (2)$$

Substituting Eq. (1) into Eq. (2), taking into account the equality $\tau(\Omega_i, s_1, s_2) = \tau(\Omega_i, s_1, s)\tau(\Omega_i, s, s_2)$, and approximating the angular integral using the Gauss quadratures gives:

$$\begin{aligned}\sum_{k=1}^{N_H} w_k \tau(\Omega_{ik}, 0, s_1) \int_{s_1}^{s_2} B\alpha\tau(\Omega_{ik}, s_1, s)ds = \bar{I}(\Omega_i) - \sum_{k=1}^{N_H} w_k I_\infty \tau(\Omega_{ik}, 0, \infty) \\ - \sum_{k=1}^{N_H} w_k \left[\int_0^{s_1} B\alpha\tau(\Omega_{ik}, 0, s)ds + \tau(\Omega_{ik}, 0, s_2) \int_{s_2}^{\infty} B\alpha\tau(\Omega_{ik}, s_2, s)ds \right]\end{aligned} . \quad (3)$$

Here N_H is the number of Gauss quadratures; w_k is the weight of the antenna gain pattern corresponding to the Gauss quadrature; s_1 and s_2 are the path lengths from the radiometer to the locations at which the ray with direction Ω_i enters and leaves the cloud.

Given a total number of m rays, Eq. (3) can be further discretized by dividing a field, which is large enough to contain the cloud, into $n=N^3$ (N^2 for a 2D slice) equal size volume pixels to yield the following matrix equation:

$$\mathbf{Ax} = \mathbf{b}, \quad (4)$$

where $\mathbf{x}^T = (\alpha_1, \alpha_2, \cdots, \alpha_n)$ is the vector of absorption coefficients; $\mathbf{b}^T = (b_1, b_2, \cdots, b_m)$, is the vector of measurements, b_i equals the right side of Eq.(3); and $\mathbf{A} = (a_{ij})$ is an mxn matrix with

$$a_{ij} = \sum_{k=1}^{N_H} w_k \tau(\Omega_{ik}, 0, s_1) \int_{s_1}^{s_2} B\varphi_j(s, \Omega_{ik}) \tau(\Omega_{ik}, s_1, s)ds . \quad (5)$$

$\varphi_j(s, \Omega_{ik})$ is nonzero only if the point (s, Ω_{ik}) is in the jth cloud pixel, and there $\varphi_j = 1$. When cloud is found in the retrieval to occupy only part of the field or the information of cloud boundary is available from other measurements like Radar, the retrieval process can be refined with a smaller field to get a better spatial resolution.

The dependence of the microwave measurements on atmospheric state variables is introduced by the absorption coefficient (Eqs. (1, 3, and 4)). In clouds, the absorption coefficient consists generally of contributions from liquid water (α_l), water vapor (α_v), and molecular oxygen (α_{O2}). The formulae for calculating absorption coefficient for non-precipitating clouds, given state variables of the atmosphere, are those of Westwater (1972) and Falcone (1966); they are also specified in the Appendix of Warner et al. (1985). The absorption coefficient is simply a linear function of LWC,

$$\alpha = \kappa_l \cdot LWC + \alpha_v + \alpha_{O2}, \tag{6}$$

where κ_l depends only on temperature, pressure, and wavelength. The radiometric characteristics of the three absorptive agents underlie the criteria for choosing the appropriate working frequency in cloud tomography - that is, a moderate emission strength of liquid water, and a weak absorption of water vapor and oxygen (Warner et al., 1985). At the frequency of 31.6 GHz (about 1 centimeter in wavelength), the contributions from water vapor and oxygen are usually one or two order less in magnitude than that of liquid water. So the requirement for accuracy of water vapor and oxygen to be known is not high in cloud tomography.

The first step in the retrieval of LWC is to solve Eq. (4) for the vector **x** of absorption coefficients, given the vector **b** of scanning microwave data. Then LWC can be easily deduced from Eq. (6). The transmission terms in Eqs. (3) and (4) are related to absorption coefficients, thus the inversion is actually non-linear. In practice, an iterative method is used to build the converged retrieval: an estimate of absorption coefficient α within the cloud is first made from the scanning data with the cloud taken to be homogeneous, and it is used to compute the matrix **A** and solve Eq. (4) for a new set of cloud absorption coefficients. Successive substitutions are performed until the set of cloud absorption coefficients converge. The speed of convergence is determined by the linearity of Eq. (4), and fortunately it is very close to linear because the dependence of transmission terms in Eq. (3) on absorption coefficients is weak for non-precipitating clouds.

3. Retrieval Method

As will become clear later, the matrix **A** in Eq. (4) has a large condition number, which indicates that the inverse problem is ill-posed (the solution is highly sensitive to any errors in measurements and/or matrix **A**). For such an ill-posed problem, an ideal, unambiguous retrieval would require the data and **A** to be free of noise and each cloud element to be scanned from all directions (Davison, 1983; Olson, 1995). Because both conditions are impossible to meet in reality, multiple solutions that satisfy the same radiometric measurements are expected, and special regularization techniques beyond the standard method of least squares are needed to deal with this problem. Furthermore,

determination of the optimal solution depends critically on the ill-posed nature of the inverse problem. However, the nature of the inverse problem and its relationship to the physical configuration of the radiometers have not been rigorously examined in previous studies. To fill this gap, this section first examines the ill-posedness of the cloud tomography, and then discusses the regularization technique to solve the corresponding ill-posed inverse problem.

3.1 SVD Examination of the Ill-posedness

The m x n matrix $\mathbf{A}$ ($m \geq n$) can be decomposed as:

$$\mathbf{A} = \mathbf{U}\boldsymbol{\Sigma}\mathbf{V}^T = \sum_{i=1}^{n} u_i \sigma_i v_i^T \,. \tag{7}$$

Here $\mathbf{U} = (u_1, u_2, \cdots, u_n)$ is an m x n orthogonal matrices containing a set of orthonormal input basis vector directions u_i for $\mathbf{A}$, and $\mathbf{V} = (v_1, v_2, \cdots, v_n)$ is an n x n orthogonal matrices containing a set of output basis vector directions v_i for $\mathbf{A}$; while $\boldsymbol{\Sigma} = \mathrm{diag}(\sigma_1, \sigma_2, \cdots, \sigma_n)$ is an diagonal matrix with the non-negative singular values ordered such that $\sigma_1 \geq \sigma_2 \geq \cdots \geq \sigma_n \geq 0$. The condition number of matrix $\mathbf{A}$ is defined as the ratio of the maximum to the minimum non-zero singular value, and its value characterizes the ill-posedness of the underlying problem (Hansen, 1998). A bigger condition number means that the problem is more ill-posed, and the solution is more sensitive to measurement noises or numeric errors.

The least squares solution of Eq. (5) then can be written as:

$$\mathbf{x}_{\mathrm{LS}} = \mathbf{V}\boldsymbol{\Sigma}^{+}\mathbf{U}^{T}\mathbf{b} = \sum_{i=1}^{n} \frac{u_i^T b v_i}{\sigma_i}, \tag{8}$$

where $\boldsymbol{\Sigma}^{+}$ is the transpose of $\boldsymbol{\Sigma}$ with every non-zero element replaced by its reciprocal, and it equals the inverse of $\boldsymbol{\Sigma}$ when **A** is square. Eq. (8) suggests that the least squares solution is a linear combination of the input and output vectors (u_i and v_i) weighted by the reciprocals of σ_i. Therefore, the number of sign changes in the elements of the input and output vectors is another characteristic feature of ill-posed problems (Hansen, 1998).

Consider as an example a stratocumulus cloud with a four-radiometer setup (described in section 4). Figure 2a shows the singular values of the corresponding matrix **A** decay gradually to a very small value with no particular gap in the spectrum. In connection with ill-posed problems, the gradual decrease of the singular values is a characteristic feature of the ill-posed problem (Hansen, 1998). The condition number for this case is 420, which provides a quantitative measure of the ill-posedness of the problem. Figure 2b reveals that the output vectors v_i tend to have more sign changes in their elements as the index i increases: no sign changes in v_1, 27 changes in v_{10}, and 64 changes in v_{100}. The same is also true for the input vectors u_i. These patterns of sign changes in the input and output vectors coincide with the characteristic features of the SVD of an ill-posed problem.

3.2 Truncated SVD and L-Curve Method

The standard least squares method, which aims to find the solution that will minimize the difference between simulated and measured data, is widely used in the inversion of well-posed problems. For such an ill-posed problem as that of the cloud tomography, existence of small singular values makes the solution derived from the standard method very sensitive to measurement noises and numeric errors, and as a result, the inevitable noises/errors make this solution unrealistic (see Eq. (8)). Furthermore, multiple solutions exist within the uncertainty of measurements (see next for the demonstration of these issues).

A good method for solving these ill-posed problems is the so-called truncated SVD method (Hansen, 1998). Unlike the standard least squares method that is equivalent to keep all the singular values, the truncated SVD method is to imposes a smoothness constraint to the solution by discarding the highly oscillating parts associated with small singular values. By doing this, the sensitivity to noises and numeric errors of the problem is reduced. Of course, the truncated SVD method reduces to standard least squares method when no singular values are in fact truncated.

The key to the truncated VSD method is to determine where to truncate the singular values. Too many truncated singular values means too much smoothness is imposed on the solution, whereas too few truncated singular values means that the noises in measurements are magnified too much in the solution. The truncating point that gives the optimal retrieval is determined using the L-curve technique discussed in Hansen (1998). The L-curve corresponding to the truncated SVD is a log-log plot of the 2-norm of the solution $\|\mathbf{x}\|^2$ versus the residual norm $\|\mathbf{Ax}-\mathbf{b}\|^2$ for all possible truncating parameters (the "truncating parameter" is defined as the percent of truncated singular

values). As illustrated in Figure 3a, the 2-norm of the solution falls precipitously when the first few small singular values are truncated, while the residual norm remains almost unchanged. When more singular values are truncated, the 2-norm of the solution stops declining and the residual norm starts to increase. The optimal truncating parameter usually corresponds to the sharp corner of the L-curve. Thus, locating the L-curve's corner is paramount. In this work, we use an algorithm similar to that in Chapter 7 of Hanesn (1998) to determine the corner but based on a numerically more stable criterion of minimum distance to the origin instead of the criterion of maximum curvature

Consider the same example as in Section 3.1, we use the truncated SVD to calculate the solution of Eq. (4). The residual error of microwave radiance keeps increasing as more singular values are truncated (Figure 3b). But the rms error of LWC shows a very different behavior - it first declines, reaching a minimum around the 10% point, followed by a rapid increase (Figure 3c). The optimal retrieval of cloud LWC is not achieved at the point where the difference between simulated and measured microwave signals is minimized, although that is the point chosen by the standard least squares method. The standard least squares method thus yields a LWC error four times higher than that from the truncated SVD method. This discrepancy indicates that the retrieval is ill-posed, and the standard least squares method cannot produce the optimal retrieval.

4. Results

The simulation experiments in Warner et al. (1985) were based on a simplified, onion-like cloud, which consists of a "juicy" central core surrounded by rings of decreasing water content toward the cloud edge. Better experiments are possible now with the emerging of 3D cloud resolving models in the intervening 20 years and allow us to examine the capability of cloud tomography to retrieve more realistic spatial patterns of cloud water content. Also, with a rigorous examination of the ill-posed nature of the retrieval problem (Section 3), we are now able to investigate the utility of more advanced retrieval methods such as the truncated SVD method in cloud tomography. Furthermore, several key factors like the physical setup of radiometers and the spatial resolution of output were not discussed in the sensitivity studies of Warner et al. (1985), although they are critical for the tomographic retrieval accuracy. We have a close examination of such factors in this section, as such a task is certainly necessary to improve the physical design of cloud tomography.

4.1 Examples of the cloud LWC retrieval

For ease of comparison with Warner et al. (1985) and of visualization, here we only show the simulations using the 2D slices of the 3D cloud fields. The cloud tomography approach has been applied to four cloud cases (see Figure 4), for four tomography setups differing with each other in either the number of radiometers or the output resolution (see Table 1). The first cloud case is an ideally homogeneous cloud with a constant LWC. The second case is an onion-like cloud with a juicy core in the center, which is similar to the "onion" distribution used in Warner et al. (1985). The third case is a stratocumulus cloud

simulated by the DHARMA large eddy simulation model driven by data from Atlantic Stratus Experiment (Ackerman et al., 1995). The fourth case is also from the DHARMA model but is a patchy cumulus situation based on Atlantic Tradewind Experiment data. The maximum and mean LWC values of each cloud case range from 0.5 to 1 gm^{-3} and 0.02 to 0.6 gm^{-3} (Table 1), respectively. The cloud field in all cases is 5000 m wide and 1500 m high, and it is digitized to the desired output resolution before simulating the radiometer measurements. In all simulations, the radiometers are equally spaced on the ground with the distance between the first and the last being 10 km.

We use relative error as a metric of retrieval quality to keep the same reference point as in Warner et al. (1985). Relative error of LWC is computed as the ratio of the rms error of LWC to the maximum LWC value within the cloud. The metric for the truncated SVD method for each combination of cloud case/tomography setup is shown in Table 1. The retrieval error from Warner's dual-radiometer setup is more than 10% for the first three cloud cases at 10 by 10 output resolution. With the four-radiometer setup, the cloud tomography method can retrieve LWC within 5% accuracy at the same spatial resolution. The eight-radiometer setup further improves the retrieval to an accuracy about 3% at 10 by 10 resolution. However, the retrieval accuracy with the eight-radiometer setup degrades to about 6% at 20 by 20 resolution. These results indicate that adding more radiometers tends to improve the tomographic retrieval, while increasing output resolution leads to the opposite direction.

The metric for the standard least squares method is shown in Table 1 in the parenthesis. The error of the standard least squares method is always higher than that of the truncated SVD method. For Setup I the error of the standard least squares method is

about 2.8 times as that of the truncated SVD, for Setup II the ratio is 2.6, for Setup III the ratio is 1.7, and for Setup IV the ratio is 4.0. Such large discrepancies suggest that the truncated SVD method is superior to the standard method in obtaining more accurate retrieval especially for the cases that have very few radiometers or high output resolution.

Figure 5 shows the retrieved fields of the four cloud cases for Setup III (4 radiometers, 10 by 10 output resolution). In all examples, the reconstructed images well capture the spatial patterns of LWC in the original images. For the homogeneous cloud case, the retrieval successfully reproduces the homogeneous field. The juicy core in the onion cloud case is correctly located in the reconstructed image. The horizontal homogeneity and vertical heterogeneity in the stratocumulus cloud case are reasonably captured by the retrieval. The retrieval also reproduces the patchy clouds in the broken cloud case. Nevertheless, the retrievals fail to reproduce most of the fine structures in the original stratocumulus and broken cumulus clouds due to the relatively coarse output resolution. Overall, the spatial patterns LWC are well reproduced by the tomographic retrievals.

An important cloud property of interest to the climate modelers is the Liquid Water Path (LWP), the vertically integrated LWC. Figure 6 suggests that the retrieved LWP compares favorably with the true LWP in 10 vertical columns of the clouds. The maximum error is approximately 20 gm^{-2}, which is similar to that of the zenith-looking MicroWave Radiometer (MWR) at the ARM sites (Liljegren et al., 2001). An apparent advantage of cloud tomography over the MWR is that LWP over multiple locations can be measured simultaneously without moving the radiometers to all these locations.

4.2 Sensitivity studies

The retrieval of cloud LWC depends on many factors. Among these are the number of radiometers, the output resolution, the number of scanning directions, and the receiver noise level. This section examines the impacts of these factors on the retrieval quality. The third cloud case (stratocumulus) is used in the sensitivity studies. If not stated, the specification of tomography setup used in the simulations is the same as Setup III (4 radiometers of 0.3 K noise level, 2 scanning angles per pixel, 10 by 10 output resolution). The 0.3 K noise level with one-second integration time is representative of the state of the art of current microwave radiometers (Westwater et al., 2004, Mittioli et al., 2005). At 10 by 10 output resolution, 2 scanning angles per pixel makes the total number of scanning angles being 200, which is approximately the number of "useful" scanning angles (those hit the retrieval field) we can get with 4 radiometers in a two-minute period.

The first factor investigated is the number of radiometers. Figure 7a depicts the representative decreasing trend of retrieval error with number of radiometers. With few radiometers, say two, adding one more improves the retrieval significantly. Warner's dual-radiometer setup is indicated by a dash-dotted line; it is clearly not optimal for retrieving the stratocumulus cloud at 10 by 10 resolution. When there are already 4 radiometers, including an additional one doesn't yield significant improvement. This suggests that the optimal number of radiometers is 4 when the desired output resolution is a few hundred meters. Our simulations show this result is also valid for the other cloud cases. The dashed curve in Figure 7a shows that condition number shares the same trend as retrieval error. Recall that a higher condition number usually means the underlying

problem is more ill-posed and thus a larger retrieval error is more likely. Retrieval becomes less ill-posed when more radiometers are used, which is consistent with the trend of retrieval error.

The next factor examined is the output resolution. Output resolution determines the finest spatial scale to be resolved. Figure 7b reveals that forcing cloud tomography to retrieve finer structure results in an increased error in the retrieved LWC. A close inspection of Figure 7b suggests that, at very coarse resolution, the retrieval problem is not ill-posed (characterized by a small condition number) and thus the retrieval error is very small. The ill-posedness of the retrieval problem keeps increasing at the region of intermediate resolution, which results in a rapid increase in the retrieval error at this region. The increase of the retrieval error becomes less rapid, though the condition number keep increasing with the output resolution after the point of 24 by 24. The reason for this is that the retrieval problem has already been very ill-posed and the best retrieval has been achieved with a big truncating parameter, in other words, the cloud field has been constrained to be almost homogeneous. The high condition number and thus large retrieval error at a high output resolution indicates that more radiometers and/or radiometers with lower noise level are needed to retrieve cloud information at such a fine scale. For a given cloud tomography setup, the choice of output resolution should be based on the desired retrieval accuracy.

Figure 7c suggests that the retrieval is more accurate when each cloud pixel is viewed from more directions. The condition number shares the same trend; it means the retrieval problem becomes less ill-posed with increasing number of scanning angles. In addition, Figure 7c indicates that beyond some point, say 3 scanning angles per pixel,

increasing the number of scanning angles is no longer a good strategy to improve LWC retrieval - both the retrieval error and the condition number level off.

The last factor is the radiometer noise level. Figure 7d shows that retrieval error increases with the radiometer noise, as one would expect. When the microwave signal is free of noise, cloud tomography reconstructs the cloud field exactly. Retrieval error first increases fast when the noise level is very low and then becomes less sensitive when the noise level is very high, while the condition number shows no variation. Since the condition number is a characteristics of only matrix **A** (see Eq. (5), **A** is weakly depended on the transmission terms in Eq. (4) therefore is a weak function of cloud liquid water), it is not surprising that the condition number does not change with the noise level at all (Figure 7d). Therefore, it is an intrinsic characteristics of the tomography setup that is determined by the output resolution, the physical arrangement and scanning strategy of the radiometers.

In summary, the retrieval accuracy is mainly determined by the physical arrangement of the radiometers, the radiometer scanning strategy, and the noise level of radiometers. Among these factors, the radiometer noise level trades off against the number of scanning angles because more scan angles means shorter dwell time for each measurement and thus larger noise. The optimal choice of these parameters can be figured out by a similar analysis to that presented in Figures 7c and 7d.

5. Concluding Remarks

The cloud tomography method has been revisited and extended, with emphasis on understanding the mathematical nature of the retrieval problem and its relationship to the physical configuration of the cloud tomography system. The retrieval problem is found to be highly ill-posed, and as a result, the standard least squares method fails to produce the optimal retrieval. Instead, the truncated SVD method is successfully used in the retrieval algorithm, and it produces more accurate retrievals than the standard method. It is also shown that retrieval of cloud LWC depends on the radiometer noise level, the total number of scanning angles, the number of radiometers, and the output resolution. Moreover, modern cloud-resolving models allow us to examine the capability of cloud tomography to retrieve more realistic cloud structure. With a cloud tomography setup consisting of 4 radiometers of 0.3 K noise level, the rms error in the reconstructed LWC image is within 5% of the maximum value of LWC present in the clouds. Overall, application of the cloud tomography method will add a great deal information to existing cloud measurements at a relatively modest cost compared to scanning radar.

The retrieval algorithms of limited angle tomography usually make use of some prior knowledge to reduce variability in the retrieval and improve the reconstructed image (Rangayyan et al., 1985). In this work, smoothness constraint has been employed in our retrieval algorithm through the truncated SVD method. Similarly, a non-negative constraint can be imposed to further reduce the function space of retrieval, and this additional constraint is likely to improve retrievals of small LWCs (Liu et al., 1999). Another potentially useful constraint is the adiabatic LWC, which provides an upper bound for the retrieval. Other measurements such as from a cloud radar or infrared

thermometer can also serve as further constraints to the retrieval algorithm. We plan to examine these issues in the future studies.

Acknowledgments

This research is supported by the DOE Atmosphere Radiation Measurement program under Contract DE-AC02-98CH10886. It is a pleasure to acknowledge the insightful discussions with Drs. Kollias Pavlos, Andy Volgemann, Mark Miller, and Richard Cederwall. The authors also thank Dr. Ed Westwater for providing the photograph of the microwave radiometers.

References

Ackerman, T., and G. Stokes (2003): The atmospheric radiation measurement program. *Physics Today*, 56, 38-45.

Ackerman, S.A., O.B. Toon, P.V. Hobbs (1995): A model for particle microphysics, turbulent mixing, and radiative transfer in the stratocumulus topped marine boundary layer and comparisons with measurements. *J. Atmos. Sci.*, 52, 1204-1236.

Davison, M.E. (1983): The ill-conditioned nature of the limited angle tomography problem. *SIAM J. Appl. Math*, 43:2, 428-448.

Drake, J.F., and J. Warner (1988): A theoretical study of the accuracy of tomographic retrieval of cloud liquid with an airborne radiometer. *J. Atmos. Sci. Ocean. Tech*., 5, 844-857.

Falcone, V. (1966): Calculation of apparent sky temperature at millimeter wavelengths. *Radio Sci*., 1 (new series), 1205-1209.

Fleming, H.E. (1982): Satellite remote sensing by the technique of computed tomography. *J. Appl. Meteorol*., 21, 1538-1549.

Flores, A., G. Ruffini, A. Rius (2000): 4D tropospheric tomography using GPS slant wet delays. *Ann. Geophys*., 18, 223-234.

Hansen, P.C. (1998): *Rank deficient and ill-posed problems: Numerical aspects of linear inversion*. SIAM J. Appl. Math., Philadelphia, pp. 247.

Hoffman, R.N., C. Grassotti, R.G. Isaacs, and T.J. Kleespies (1989): A simulation study of satellite emission computed tomography. *J. Appl. Meteorol*., 28, 321-342.

Hogan, R. J., N. Gaussiat and A. J. Illingworth (2005): Stratocumulus liquid water content from dual-wavelength radar. *J. Atmos. Oceanic Technol.,* 22, 1207-1218.

Hogg, D.C., F.O. Guiraud, J.B. Snider, M.T. Decker , and E.R. Westwater (1983): A steerable dual-channel microwave radiometer for measurement of water vapor and liquid in the troposphere. *J. Appl. Meteorol*., 22, 789–806.

Lawson, C.L., and R.J. Hanson (1974): *Solving least squares problems*. Prentice-Hall, Englewood Chffs, NJ, 158-169.

Liljegren, J., E. Clothiaux, G. Mace, S. Kato, and X. Dong (2001): A new retrieval for cloud liquid water path using a ground-based microwave radiometer and measurements of cloud temperature, *J. Geophys. Res*., 106, 14,485-500.

Liu, Y., W.P. Arnott, and J. Hallett (1999): Particle size distribution retrieval from multispectral optical depth: Influences of particle nonsphericity and refractive index. *J. Geophys. Res*., 104:31, 753-762.

Mattioli, A., E.R. Westwater, S.I. Gutman, and V.R. Morris (2005): Forward model studies of water vapor using scanning microwave radiometers, global positioning system, and radiosondes during the cloudiness intercomparison experiment. *IEEE Trans. Geosci. Remote Sens*., 43, 1012-1023.

Olson, T. (1995): A stabilized inversion for limited angle tomography. *IEEE Eng. Med. Biol*., 14, 612-620.

Rangayyan, R., A.P. Dhawan, and R. Gordon (1985): Algorithms for limited view computed tomography - An annotated bibliography and a challenge. *Appl. Opt*., 24, 4000-4012.

Stephens, G.L. (2005): Cloud feedbacks in the climate system: a critical review. *J. Climate*, 18, 237-273.

Twomey, S. (1987): Iterative nonlinear inversion methods for tomographic problems. J. *Atoms. Sci*., 44, 3544-3551.

Warner, J., J.F. Drake, and P.R. Krehbiel (1985): Determination of cloud liquid water distribution by inversion of radiometric data. *J. Atmos. Sci. Ocean. Tech*., 2, 293-303.

Warner, J., J.F. Drake, and J.B. Snider (1986): Liquid water distribution obtained from coplanar scanning radiometers. *J. Atmos. Sci. Ocean. Tech*., 3, 542-546.

Warner, J., and J. F. Drake (1988): Field tests of an airborne remote sensing technique for measuring the distribution of liquid water in convective cloud. *J. Atmos. Oceanic Technol*., 5, 833–843.

Westwater, E.R. (1972): Microwave emission from clouds. NOAA Tech. Rep. ERL 219-WPL, 18, pp. 43.

Westwater, E.R., S. Crewell, and C. Matzler (2004): A review of surface based microwave and millimeter wave radiometric remote sensing of the troposphere. *Radio Sci. Bull*., 3010, 59-80.

Wiscombe, W.J. (2005): *Scales, tools, and reminiscences*. In A. Marshak and A.B. Davis (Eds.), Three-dimensional radiative transfer in the cloudy atmosphere, Springer-Verlag, 3-92.

Table

Table 1. Relative error of the LWC retrieved by the truncated SVD method for each of the following four cloud tomography setups and four cloud cases. The tomography setups are different with each other in either number of radiometer or output resolution. The cloud fields are 5000 m wide and 1500 m high. Since the radiometer noise is a random function from ray to ray, the relative error metric is computed as the mean relative error from 10 runs for each combination of cloud case/setup. The values in the parenthesis correspond to the standard least squares method.

Cloud cases	**Max LWC, gm^{-3}**	**Mean LWC, gm^{-3}**	**Relative errors**			
			Setup I	**Setup II**	**Setup III**	**Setup IV**
			2 radiometers 10x10 pixels	**4 radiometers 10x10 pixels**	**8 radiometers 10x10 pixels**	**8 radiometers 20x20 pixels**
Homogeneous	0.60	0.60	12%(32%)	5%(17%)	3%(5%)	5%(28%)
Onion	0.50	0.20	13%(26%)	5%(15%)	3%(6%)	6%(24%)
Stratocumulus	0.97	0.23	14%(27%)	5%(11%)	3%(5%)	8%(22%)
Broken cumulus	1.0	0.03	7%(33%)	4%(8%)	3%(4%)	6%(21%)

*The values in the parenthesis correspond to the standard least squares method.

Figures

Figure 1: A comparison of the scanning microwave radiometer used in Warner et al. (1986) for a cloud tomography demonstration (top) with the radiometers deployed in Barrow, Alaska, USA during 2004 (bottom). The radiometers used by Warner et al. operates at two frequencies (23.8 and 31.4 GHz). The scanning bearings are on the top of the trailer; the electronics and antenna are located in the trailer to keep a benign working environment. MicroWave Radiometer (MWR, the photo is enlarged three times) is a dual-frequency (23.8 and 31.4 GHz) radiometer and is used to measure vertically integrated water contents. Ground-based Scanning Radiometer (GSR) is a multi-frequency scanning radiometer operating from 50 to 380 GHz; it can provide unprecedented information on the evolution of temperature, water vapor, and clouds. The photo shows the scanhead moved out of the framework for atmospheric viewing. The circles are the radiometers of different wavelengths mounted on the scanhead.

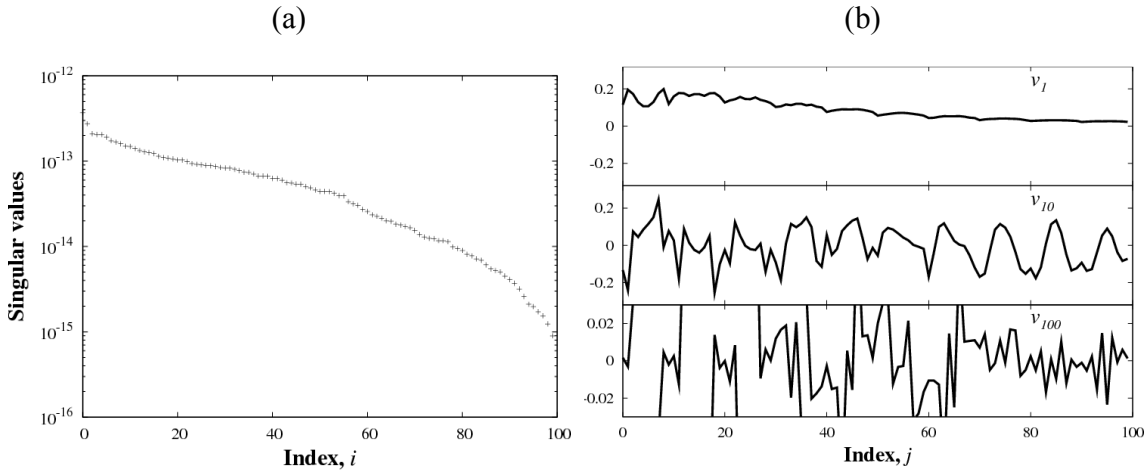

Figure 2: The singular value decomposition of the matrix **A** for the tomographic retrieval problem described in Section 3.1. (a) The singular values decay to almost zero as the index i increases. (b) The output vectors v_i have more sign changes in their elements as the index i increases. There is no sign changes in the first output vector v_1, while there are 27 sign changes in v_{10} and 64 sign changes in the last output vector v_{100}.

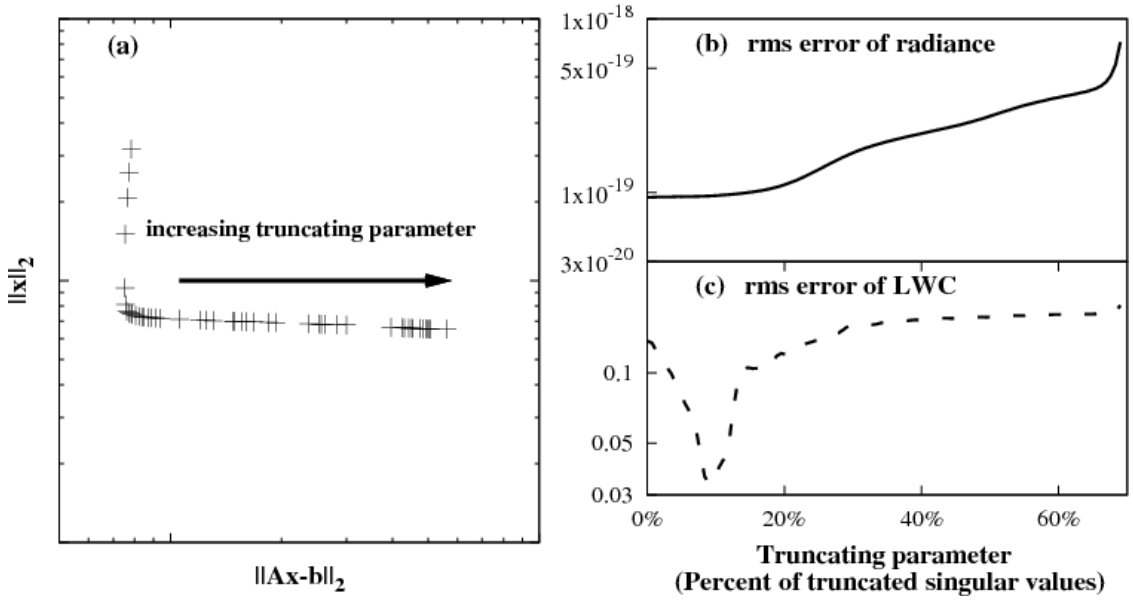

Figure 3: The illustration of obtaining optimal retrieval of LWC through the truncated SVD method. (a) Schematic illustration of the L-curve. The corner of the L-curve is usually not far from the point which gives the optimal reconstruction. (b) The rms error of microwave radiance as a function of truncating parameter defined as percent of singular values that are neglected in the retrieval algorithm. The standard least squares method corresponds to the case that the truncating parameter is zero. (c) is the same as (b), but for the rms error of the retrieved LWC. The rms error of LWC from the standard least squares method is 4 times higher than that from the truncated SVD method.

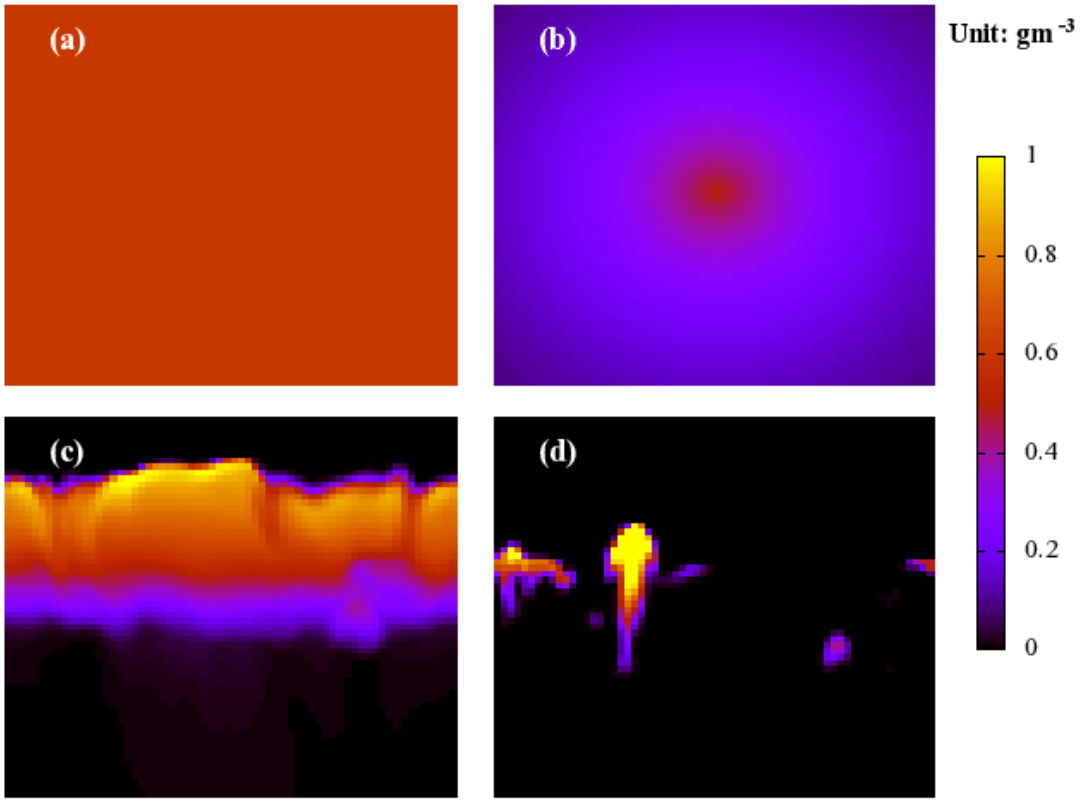

Figure 4: The liquid water fields of the following four cloud cases: (a) homogeneous cloud, (b) onion cloud, (c) stratocumulus cloud, (d) broken cumulus cloud.

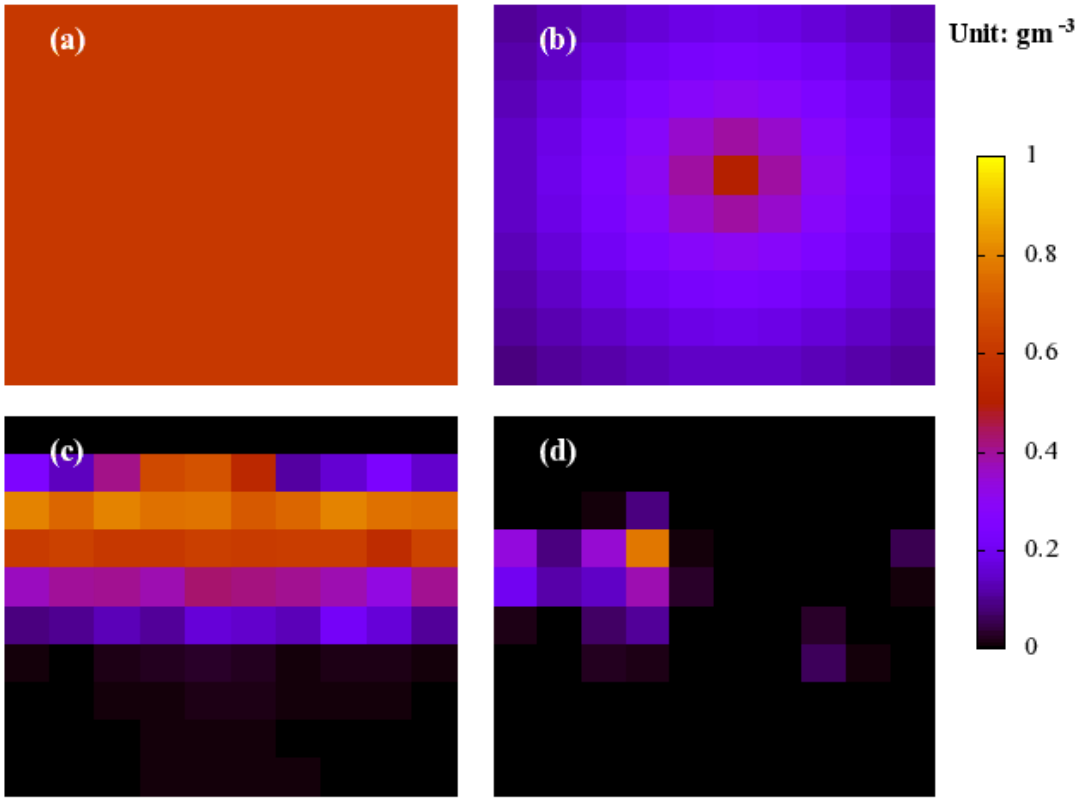

Figure 5: The retrieved LWC fields for the afore-mentioned cloud cases using cloud tomography Setup III (4 radiometers of 0.3 K noise level, 2 scanning angle per pixel, 10 by 10 output resolution). (a) homogeneous cloud, (b) onion cloud, (c) stratocumulus cloud, (d) broken cumulus cloud.

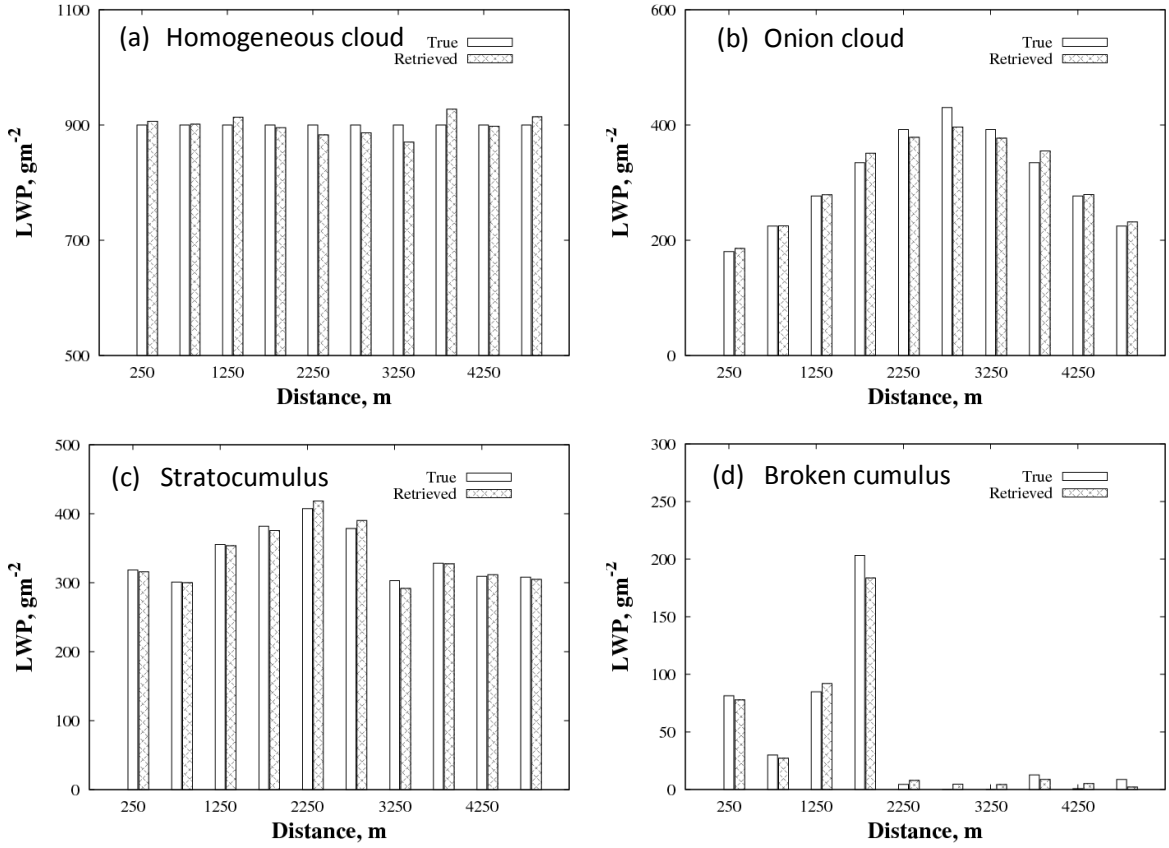

Figure 6: The comparison of the true LWP as a function of location with the LWP computed from the liquid water fields retrieved with the tomography setup III for the following cloud cases: (a) homogeneous cloud, (b) onion cloud, (c) stratocumulus cloud, (d) broken cumulus cloud.

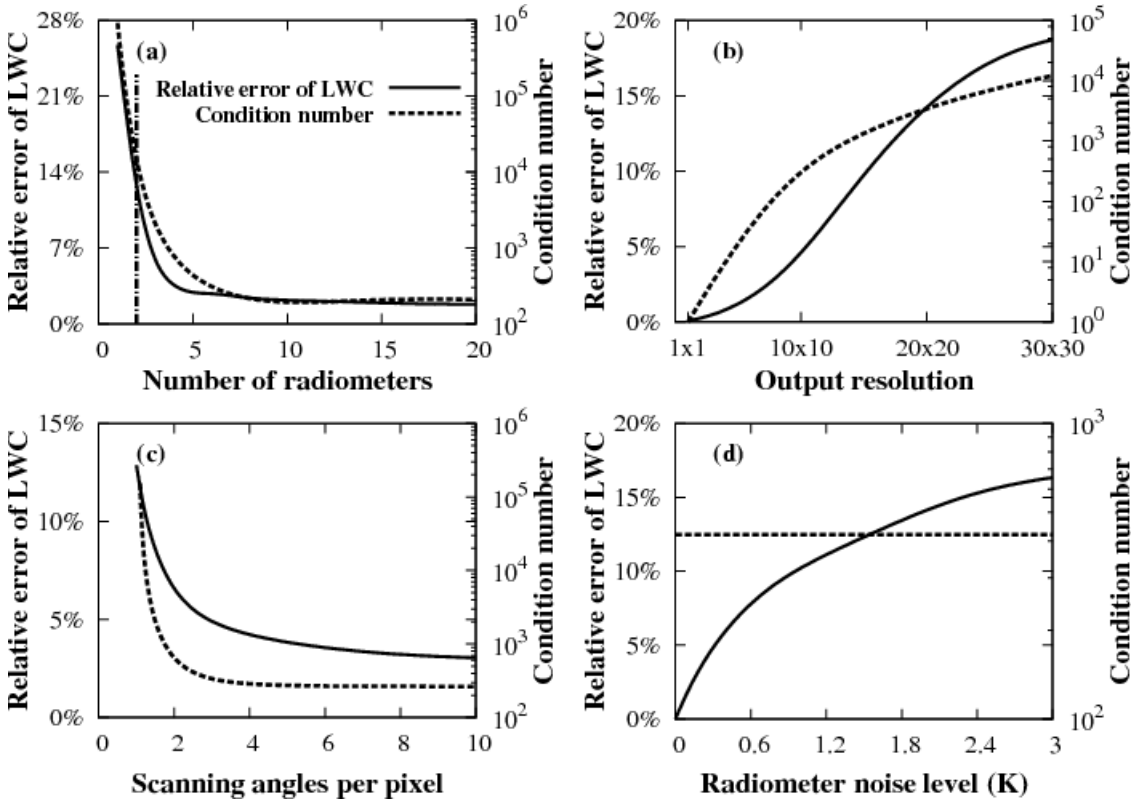

Figure 7: The relative error of retrieved LWC as a function of (a) the number of radiometers, (b) the output resolution, (c) the number of scanning angles per pixel, and (d) the radiometer noise level. Warner's dual-radiometer setup is indicated by a vertical dash-dotted line in (a).